NIH Public Access
Author Manuscript
J Pept Res. Author manuscript; available in PMC 2006 March 20.

Published in final edited form as:
J Pept Res. 2005 February ; 65(2): 209–220.

Stability and specificity of heterodimer formation for the coiled-coil neck regions of the motor proteins Kif3A and Kif3B: the role of unstructured oppositely charged regions

M.S. Chana, **B.P. Tripet**, **C.T. Mant**, and **R. Hodges**
Department of Biochemistry and Molecular Genetics, University of Colorado Health Sciences Center at Fitzsimons, Aurora, CO, USA

Abstract

We investigated the folding, stability, and specificity of dimerization of the neck regions of the kinesin-like proteins Kif3A (residues 356–416) and Kif3B (residues 351–411). We showed that the complementary charged regions found in the hinge regions (which directly follow the neck regions) of these proteins do not adopt any secondary structure in solution. We then explored the ability of the complementary charged regions to specify heterodimer formation for the neck region coiled-coils found in Kif3A and Kif3B. Redox experiments demonstrated that oppositely charged regions specified the formation of a heterodimeric coiled-coil. Denaturation studies with urea demonstrated that the negatively charged region of Kif3A dramatically destabilized its neck coiled-coil ($urea_{1/2}$ value of 3.9 M compared with 6.7 M for the coiled-coil alone). By comparison, the placement of a positively charged region C-terminal to the neck coiled-coil of Kif3B had little effect on stability ($urea_{1/2}$ value of 8.2 M compared with 8.8 M for the coiled-coil alone). The pairing of complementary charged regions leads to specific heterodimer formation where the stability of the heterodimeric neck coiled-coil with charged regions had similar stability ($urea_{1/2}$ value of 7.8 M) to the most stable homodimer (Kif3B) with charged regions ($urea_{1/2}$ value of 8.0 M) and dramatically more stable than the Kif3A homodimer with charged regions ($urea_{1/2}$, value of 3.9 M). The heterodimeric coiled-coil with charged extensions has essentially the same stability as the heterodimeric coiled-coil on its own ($urea_{1/2}$ values of 7.8 and 8.1 M, respectively) suggesting that specificity of heterodimerization is driven by non-specific attraction of the oppositely unstructured charged regions without affecting stability of the heterodimeric coiled-coil.

Keywords

coiled-coil; heterodimerization; Kif3; kinesin; protein stability; unstructured charged regions

Kinesin superfamily proteins are microtubule-activated ATPases that share homology in their microtubule binding/ ATP hydrolyzing motor domains. Conventional kinesin is the most studied member of the superfamily and has been shown to be composed of two heavy and two light chains (1–3). The second protein in the kinesin superfamily of proteins to be completely characterized was found to be a heterotrimeric complex composed of two large subunits with microtubule-activated ATPase activity similar to conventional kinesin heavy chains and an accessory protein (Fig. 1) (4). This heterotrimeric protein was termed kinesin-II but is also called the Kif3 complex, where Kif represents the kinesin family (5).

Correspondence to: *Robert Hodges*, Department of Biochemistry and Molecular Genetics, University of Colorado Health Sciences Center at, Fitzsimons, Aurora, CO 80045, USA, Tel.: (303) 724-3253, Fax: (303) 724-3249 E-mail: robert.hodges@uchsc.edu

NIH-PA Author Manuscript
NIH-PA Author Manuscript
NIH-PA Author Manuscript

NIH-PA Author Manuscript

NIH-PA Author Manuscript

NIH-PA Author Manuscript

The sequence identification and characterization for the subunits of the Kif3 complex, isolated from sea urchin, have been completed. The 85-kDa subunit was the first to be characterized and was termed spKRP85 (for *Strongylocentrotus purpuratus* kinesin related protein 85 kDa) (6). The characterization of the mouse protein homolog Kif3A has also been reported (7). In 1995, the sequence of the 95-kDa subunit found in sea urchin, termed spKRP95, was published (8), followed by the sequence publication of its mouse homolog, Kif3B(9). The accessory proteins in sea urchin and mouse were sequenced and reported in 1996 (4,5). These proteins have since been named kinesin-like associated proteins (KAPs). Within the same organism, spKRP85 was found to have 52% sequence identity with the full-length spKRP95, and 73% within the motor region. Kif3A and Kif3B were found to have 47% sequence identity along their full length and 61% in their motor regions.

Upon analysis of the spKRP85/95 and Kif3A/B motor subunits, it was noted that the NH_2 termini (approximately residues 1–350) were likely, based on sequence homology, to comprise a motor domain similar to conventional kinesin. The NH_2 terminal domains were predicted to be separated from the small globular COOH-terminal domains by a central α-helical segment thought to form a coiled-coil similar to the one shown for conventional kinesin (Fig. 1) (10). A similar stalk-like structure as seen for conventional kinesin was noted for the Kif3A/B complex in electron micrographs (9). Interestingly, in the similarity profiles between spKRP85/Kif3A and spKRP95/Kif3B, a small portion of sequence was found to have strikingly low sequence homology and was not predicted to form a coiled-coil. This region was located in the sequence between the neck and stalk regions (Fig. 1) and had low probability for α-helix formation (6,8,9). This region is referred to as the hinge region (Fig. 1). When these regions were further scrutinized, it was noted that spKRP85/Kif3A had a stretch of amino acids with a number of negatively charged amino acids closely spaced (11 and 13 negatively charged amino acids in spKRP85 and Kif3A, respectively). This negatively charged segment was found to be followed by a segment of positively charged amino acids (nine in both proteins). This region of sequence disparity in spKRP95/Kif3B was found to begin with a stretch of positively charged amino acids (eight in each protein) followed by a segment of negatively charged amino acids (11 and 14 in spKRP95 and Kif3B, respectively) (Fig. 1). It was postulated that these complementary charged regions in the hinge region could help the motor subunits form spKRP85/95 and Kif3A/B heterodimers through the destabilization of homodimers, and stabilization of heterodimers through electrostatic attractions (8). It was also noted that polar and charged residues were found in the stalk region **a** and **d** positions of the coiled-coil (8). The **a** and **d** positions are classically reserved for hydrophobic residues in a coiled-coil (11), and it was predicted that the formation of heterodimers would prevent electrostatic repulsions in the hydrophobic core of the coiled-coil stalk region of the homodimeric proteins (8). Support for the possible role of **a** and **d** positions in the stalk region in heterodimer formation has been bolstered by a recent study (12), where the ability of the C-terminal heptads of the stalk domain to form heterodimers was demonstrated.

In our efforts to characterize the neck region coiled-coil and complementary charged regions (hinge region; Fig. 1) of the motor proteins Kif3A and Kif3B, we analyzed the ability of each neck region to form a coiled-coil on its own (13,14). Previously, we focused on the effects of complementary charged regions on the formation of the homodimeric coiled-coils of Kif3A and Kif3B (13,14); i.e. the coiled-coil segment was homodimeric but, with oppositely charged regions attached, the molecules were heterostranded. We demonstrated that the negatively charged segments of both Kif3A and Kif3B charged regions, when attached directly to the neck region coiled-coils, destabilized their respective neck region coiled-coils, while, in contrast, the positively charged segments did not affect the stability of the coiled-coil neck regions. Furthermore, it was shown that a negative and positive charged extension was required to specify heterostranded coiled-coil formation in the presence of identical coiled-coil sequences.

NIH-PA Author Manuscript

NIH-PA Author Manuscript

NIH-PA Author Manuscript

In the present study, we examine the formation of heterodimeric molecules of Kif3A and Kif3B, where both the coiled-coil regions and the charged segments represent the sequences found in native Kif3A and Kif3B. These results allowed us to determine the role of the complementary charged regions in determining the specificity and stability of the heterodimeric Kif3A/Kif3B coiled-coil.

Experimental Procedures

Synthesis of peptides

Peptides were synthesized on a 4-methylbenzhydrylamine (MBHA) hydrochloride resin using conventional N^{α}-*t*butyloxycarbonyl (*t*-Boc) chemistry and standard solidphase synthesis methodology (15,16). Each coupling step used a four times excess of amino acid per free amino group on the resin with 2-(1H-benzotriazole-1-yl)-1,1,3,3- tetramethyluranium hexafluorophosphate (HBTU)/*N*-hydroxybenzotriazole (HOBT) activation. The extent of each coupling was determined by conducting a Kaiser test (17) on a small sample of resin. An additional coupling was performed if the coupling reaction was <99% complete. Acetylation was used to terminate any unreacted amino groups from the coupling step as well as the final N^{α}-amino group of the polypeptide chain. Cleavage of the peptide from the resin and deprotection of the side-chain-protecting groups was achieved using a low trifluoromethanesulfonic acid (TFMSA) and high hydrogen fluoride (HF) procedure for 3 and 1.5 h, respectively (18). HF was removed under vacuum and the peptide-resin was washed several times with cold ether. The peptide was dissolved and extracted by filtration from the resin using a 50 : 50 mixture (v/v) of acetonitrile : water containing 0.05% aqueous trifluoroacetic acid (TFA) and lyophilized.

Peptide purification

Purification of each peptide was performed by reversed-phase high-performance liquid chromatography (RP-HPLC) on a Varian 5000 Liquid Chromatograph (Varian, Walnut Creek, CA, USA) using an Aquapore RP-300 C8 column [250 × 7.0 mm internal diameter (i.d.), 7 μm particle size, 300 Å pore size; Applied Biosystems, Foster City, CA, USA] with a linear AB gradient (ranging from 0.2% to 1.0% B/min) at a flow rate of 2 mL/min, where solvent A is aqueous 0.1% TFA and solvent B is 0.1% TFA in aceto-nitrile. The column was kept at 80 °C throughout the duration of the purification using a column heater.

Amino acid analysis

Purified peptides were hydrolyzed in 6 $_{N}$ HCl containing 0.1% phenol for 1.5 h at 160 °C in evacuated, sealed tubes. Amino acid analysis was performed on a Beckman model 6300 amino acid analyzer (Beckman Instruments, Berkeley, CA, USA).

Mass spectrometry

The correct molecular masses of the purified peptides and proteins were confirmed by electrospray mass spectrometry using a Mariner electrospray ionization time of flight mass spectrometer (Applied Biosystems) calibrated with horse heart myoglobin (mass 16, 951.51). The molecular masses were determined with an uncertainty of ±2–3 Da.

Circular dichroism spectroscopy

Circular dichroism (CD) spectra were recorded on a Jasco J-810 spectropolarimeter (Jasco Inc., Easton, MD, USA). The temperature-controlled cuvette holder was maintained at the desired temperature with a circulating water bath. The instrument was calibrated with an aqueous solution of recrystallized d-10(+)-camphorsulfonic acid at 290.5 nm. Results were expressed as mean residue molar ellipticity [θ] (deg cm^2/dmol) calculated by using the equation

NIH-PA Author Manuscript

NIH-PA Author Manuscript

NIH-PA Author Manuscript

$$[\theta] = \frac{\theta_{obs} - MRW}{10lc}$$

where, θ_{obs} is the observed ellipticity expressed in millidegrees, MRW the mean residue molecular weight (molecular weight of the peptide divided by the number of amino acids), *l* the optical path length in centimeters, and *c* the final peptide concentration in milligrams per milliliter. For wave scans, data were collected from 190 to 255 nm at 0.05-nm intervals, and the average of 10 scans reported. GdnHCl and urea denaturation studies were carried out by preparing mixtures of a stock solution of peptide in buffer (0.1 M KCl, 0.05 M K_2HPO_4/KH_2PO_4, pH 7), buffer alone and a solution of 8 M GdnHCl or 10 M urea in buffer, where the ratios of buffer and 8 M GdnHCl or 10 M urea solutions were varied to give the appropriate final GdnHCl or urea concentrations. All peptide concentrations were determined by amino acid analysis.

Protein unfolding measurements

Denaturation midpoints: $GdnHCl_{1/2}$, and $urea_{1/2}$ values for the disulfide-bridged peptides were determined by following the change in molar ellipticity at 222 nm. Ellipticity readings for GdnHCl and urea denaturations were normalized to the fraction of the peptide population that was folded (f_f) using the standard equation

$$f_f = \frac{[\theta] - [\theta]_u}{[\theta]_n - [\theta]_u},$$

where $[\theta]_n$ and $[\theta]_u$ represent the ellipticity values for the fully folded and fully unfolded peptide population, respectively. [θ] is the observed ellipticity at 222 nm at any denaturant concentration.

Preparation of oxidized peptides

Formation of homo-two-stranded disulfide-bridged molecules was carried out by dissolving 5 mg of each peptide in 2 mL of 100 m M NH_4HCO_3, pH 8, buffer and the reaction vessel stirred overnight at room temperature. Oxidized peptides were re-purified by RP-HPLC and oxidation verified by mass spectrometry.

Redox experiments

Redox experiments were carried out in a similar manner to that described previously (19,20), with modifications as indicated. Disulfide-bridged, homo-two-stranded peptides were mixed together from stock concentrations to final concentrations of 100 μ M each in 0.1 M KCl, 0.05 M K_2HPO_4/KH_2PO_4, pH 7.0 buffer and degassed by blowing steady stream of N_2 through the buffer for 16 h. The reactions were carried out at room temperature in Reacti vials Chromatographic Specialties, Inc., Brockville, ON, Canada). The peptides were then mixed in a 1 : 1 ratio in the presence of a 10 times molar excess of reduced and oxidized glutathione. At set time intervals, 15-μL aliquots were taken from the Reacti vials and the reaction was quenched by the addition of either 10 μL of 3% aq. phosphoric acid or 10 μL of 5% TFA. Each aliquot was then injected onto a Zorbax 300SB-C8 column (150 × 2.1 mm i.d., 5-μm particle size, 300-Å pore size; Agilent Technologies, Little Falls, DE, USA) and eluted with a 1% acetonitrile/min gradient to assess the ratios of disulfide-bridged homostranded and heterostranded peptides in the reaction mixture.

NIH-PA Author Manuscript

NIH-PA Author Manuscript

NIH-PA Author Manuscript

Results

Secondary structure of the complementary charged regions of Kif3A and Kif3B

The complementary charged regions we have investigated are those of Kif3A (residues 378–416) and Kif3B (residues 373–411). We synthesized two peptides to represent these regions (P5 and P10, respectively) (Fig. 1). CD analysis of the peptides showed that, on their own and mixed equally at a 1 : 1 molar ratio, they did not adopt any secondary structure (Fig. 2A); i.e. the CD spectrum of each sample was similar to a random coil spectrum. When the peptides were linked by a disulfide bond at the N-terminus using a flexible CGG linker, to remove the concentration dependence, the peptides still did not adopt any detectable defined secondary structure. The oxidized (disulfide-linked) peptides P5, P10 and the heterostranded peptide P5/P10 all showed a spectrum characteristic of a random coil peptide (Fig. 2B).

Folding of neck-region coiled-coil

We next characterized the neck-region coiled-coil of Kif3A, Kif3B and Kif3A/B to compare and contrast differences between the homostranded and heterostranded neck regions. The sequences for peptide P2 (Kif3A residues 356–377) and peptide P7 (Kif3B residues 351–372) are shown in Fig. 3 (top and bottom panels). The CD spectrum of disulfide-bridged P2/P7 (Fig. 4A) was characteristic of a fully folded α-helical coiled, based upon the following characteristics: high molar ellipticity value in benign medium, double minima at 208 and 222 nm, and a maximum at 190 nm; an α-helical content of 100% and 22 calculated α-helical residues of 22 (Table 1); the addition of 50% trifluoroethanol (TFE) did not increase the α-helical content (determined at 222 nm) (Table 1); the $[\theta]_{222}/[\theta]_{208}$ ratio in benign medium (1.05) is characteristic of coiled-coils, i.e. >1.0 (23) and this value decreased to 0.86 in the presence of the helix-inducing solvent TFE. Although TFE stabilizes the helical secondary structure, it denatures tertiary and quaternary structure, i.e. the coiled-coil is dissociated to single-stranded α-helices as clearly demonstrated by high-performance size-exclusion chromatography of coiled-coils (19,24–27). In Fig. 4A, the spectrum of the oxidized heterostranded peptide P2/P7 is compared with the spectra of the oxidized homostranded peptidesP2 and P7. The values observed by CD spectroscopy for the heterostranded and homostranded peptides are shown in Table 1. The heterostranded peptide shows an increased α-helical content and complete folding compared to the two homostranded peptides. The flexible Cys-Gly-Gly linker was used to link peptides P2 and P7 to ensure that we were exclusively analyzing the heterostranded peptide.

Role of complementary charged regions in dimer formation

To understand the role of charged regions on specificity and stability of the heterodimeric coiled-coil, we synthesized a series of peptides derived from the neck-hinge region (Fig. 3). The top panel of Fig. 3 shows the native sequence taken from Kif3A; the neck region coiled-coil-forming residues are boxed in the native sequence and depicted beneath each of the synthetic peptides. The residues found in the hydrophobic '**a'** and '**d'** positions are shown in bold. The individual charged extensions added C-terminally are depicted by the boxes containing '−' and '+' signs, representing the charged amino acids. Similarly, the bottom panel shows the native Kif3B and derived peptide sequences.

In our previous studies, we showed the need for both positively and negatively charged regions to be present in order to specify the formation of heterostranded peptide (13), and that the stability of the coiled-coil could affect the rate of heterostranded peptide formation when the starting peptides were homostranded (14). In the present study, the results of redox equilibrium experiments (see Methods) showed that the presence of charged extensions C-terminal to the coiled-coil-forming sequences can specify the formation of a truly heterodimeric coiled-coil (Fig. 5, reactions A, B, C). Notice that the presence of two segments of complementary charged

NIH-PA Author Manuscript

NIH-PA Author Manuscript

NIH-PA Author Manuscript

regions C-terminal to the coiled-coils behave similarly (Fig. 5, reaction A) to one segment of complementary charge (Fig. 5, reactions B and C) in specifying heterostranded coiled-coil formation. The absence of charged regions leads to the formation of only 50% heterodimer, a value expected for random exchange of polypeptide strands (Fig. 5, reaction D), i.e. no specificity for heterodimer formation. In this study, we tested the ability of the complementary charged region found in Kif3A and Kif3B to specify formation of heterostranded coiled-coil in the presence of 3 M NaCl (Fig. 6). We see that in redox buffer (20,21) containing 3 M NaCl there was a decreased ability of the charged regions to contribute to the formation of heterostranded coiled-coil, producing only approximately 60% (Fig. 6) heterostranded coiled-coil product instead of the original 95% (Fig. 5). The percentage of heterostranded coiled-coil formed approaches the amount formed by random mixing of the coiled-coils without charged extensions in 3 M NaCl (Fig. 6, reaction D).

Effect of complementary charged regions on coiled-coil stability

To assess how the stability of the heterostranded coiled-coil is affected by adding complementary charged extensions in comparison to the homostranded coiled-coils of Kif3A and Kif3B, that have repulsive charged extensions, we denatured the α-helical structure of the neck coiled-coil using the chemical denaturants GdnHCl and urea. Since GdnHCl masks electrostatic interactions, repulsions and attractions (28), the denaturation midpoints of the disulfide-bridged homostranded peptides P2 and P7 and the disulfide-bridged heterostranded peptide P2/P7 will be a reflection of the stability of the coiled-coils' hydrophobic cores (Fig. 4B;Table 2A). The denaturation midpoint value of the heterostranded peptide P2/P7 (3.6 M) is approximately intermediate between the values for the homostranded peptides (P2, 3.1 M and P7, 3.9 M;Fig. 4B;Table 2A). Urea, an uncharged denaturant, does not mask electrostatic interactions (28) and so the stability results will reflect the combined effect of the hydrophobic interactions in the hydrophobic core and the effect of charged regions on the stability of the coiled-coil. As there are no charged extensions on peptides P2 and P7, the denaturation midpoints of these coiled-coils in urea will reflect the stabilities of the coiled-coils alone and this serves as our control experiment. Again the stability of the heterostranded P2/P7 coiled-coil (8.1 M; Fig. 4C; Table 2A) is approximately intermediate between the values of the two homostranded coiled-coils, P2 and P7 (P2, 6.7 M and P7, 8.8 M; Fig. 4C; Table 2A).

For peptides with only one segment of the complementary charged region added C-terminally to the coiled-coil-forming sequences, peptides P3 and P8, we expect a relative stability pattern in GdnHCl between the homostranded and heterostranded peptides to be similar to the stability pattern for the coiled-coils alone, because, as noted above, GdnHCl masks electrostatic interactions. The stability of the heterostranded P3/P8 in GdnHCl, was slightly higher than the expected midpoint (3.5 M; Fig. 7A; Table 2B, compared with a theoretical 3.3 M). The denaturation midpoint values of the homostranded peptides P3 and P8 in GdnHCl were 2.8 M and 3.7 M, respectively (Fig. 7A and Table 2B). In urea, where the effects of the charged region interactions can be observed, it would be expected that the value for the heterostranded peptide would not lie intermediate between the values of the two homostranded peptides. In fact, the hetero- two-stranded peptide (P3/P8) exhibited a coiled-coil stability ($urea_{1/2}$ value of 7.6 M) closer to the most stable homostranded peptide P8 (8.2 M; Fig. 7B; Table 2B). A urea denaturation midpoint value that came half way between the values of the two homostranded peptides (3.9 and 7.6 M) would be 5.8 M. The heterostranded peptide is considerably more stable than the homostranded peptide P3 (compare $urea_{1/2}$ values of 7.6 and 3.9 M, respectively).

Finally, for the peptides that incorporate the full-length charged region found in Kif3A and Kif3B, peptides P1 and P6 (Fig. 3), the GdnHCl midpoint value of the heterostranded P1/P6 (3.1 M; Fig. 8A; Table 2C) came between the GdnHCl midpoint values for the homostranded peptides P1 and P6 (2.7 M and 3.6 M, respectively). In urea, we see that the heterostranded peptide

NIH-PA Author Manuscript

NIH-PA Author Manuscript

NIH-PA Author Manuscript

(P1/P6) again exhibited a stability ($urea_{1/2}$ value of 7.8 M) similar to the most stable homostranded peptide P6 (8.0 M; Fig. 8B, Table 2C). The heterostranded peptide P1/P6 is substantially more stable than the homostranded peptide P1 (compare $urea_{1/2}$ values of 7.8 and 3.9 M, respectively).

Discussion

We have explored how the structure, stability and specificity effect of the charged hinge regions affect heterodimer formation of the neck region coiled-coil found in the heterotrimeric motor protein complex Kif3A/Kif3B. The complementary charged regions alone (residues 378–416 and 373–411 for Kif3A and Kif3B, respectively) were examined by CD spectroscopy and found to adopt a random coil structure by themselves and when mixed together in a 1 : 1 molar ratio. Furthermore, the charged regions were not induced into any secondary structure when attached to the neck coiled-coil regions (data not shown). Peptides, including the neck coiled-coil and the complementary charged regions (residues 356–416 and 351–411 for Kif3A and Kif3B, respectively) were studied in their disulfide-bridged form (CGG linker added to the N-terminus) either as homo- or hetero-two-stranded peptides. To assess the ability of the complementary charged regions to specify heterodimer formation of a coiled-coil, we mixed disulfide-bridged homo-two-stranded Kif3A and Kif3B peptides with their respective charged regions attached, in redox buffer (20,21). Contrary to recent findings (12), where it was suggested that the charged regions were not necessary for heterodimer formation, we observed that oppositely charged regions specified the formation of a hetero-two-stranded peptide (Figs 3 and 5, reactions A, B, C). Furthermore, mixing the disulfide-bridged Kif3A neck coiled-coil together with the disulfide-bridged Kif3B neck coiled-coil led to a 1 : 2 : 1 ratio of Kif3A homostranded : Kif3A/B heterostranded : Kif3B homostranded peptides, the ratio expected from a non-specific random pairing of peptides (Fig. 5 reaction D). The ability of the complementary charged extensions on the C-terminus of the neck coiled-coil of the two proteins to form preferentially a heterostranded peptide was diminished through charge screening in the presence of NaCl (Fig. 6). Similar charge screening by salt has been reported elsewhere (29,30).

To assess how complementary charged extensions may affect the stability of the heterodimeric neck coiled-coils in comparison to the homodimeric coiled-coils, we denatured the peptides in urea, a denaturant shown to reveal the effects of electrostatics on protein stability (31–34). The results indicate that for the neck region coiled-coils alone, the heterodimeric coiled-coil made up of the neck regions of both Kif3A and Kif3B has an intermediate stability between the homodimeric neck coiled-coils (Fig. 4C, Table 2A). With complementary charged regions added to the C-terminus of the heterodimeric neck region coiled-coil, the stability of the coiled-coil is increased relative to the intermediate stability position and is similar to the stability of the more stable homodimeric neck region of Kif3B (Fig. 7B, Table 2C).

In accordance with the original postulate (8) for the functional role of the complementary charged regions in the Kif3 complex, we see that complementary charged regions can specify hetero-two-stranded coiled-coil formation. The results of this study and our previous investigations (13,14) show the effects of the charged extensions on the stability of the coiled-coil regions. Thus, the pairing of negatively charged regions directly C-terminus to the coiled-coil led to a dramatic decrease in stability of the homostranded Kif3A neck region, while the pairing of positively charged regions did not decrease the stability of homostranded Kif3B neck region (compare Table 2A and 2B) (13,14). Thus, the formation of the heterostranded Kif3A/3B coiled-coil with a negatively charged extension on Kif3A and a positively charged extension on Kif3B prevents the destabilization observed for the homostranded Kif3A neck region while maintaining the stability similar to that of the homostranded Kif3B. Interestingly, adding a second oppositecharged segment to the first charged extension already present on

NIH-PA Author Manuscript

NIH-PA Author Manuscript

NIH-PA Author Manuscript

either Kif3A or Kif3B had no effect on the stability of the homodimeric coiled-coils (Table 2B,C). Correspondingly, the heterostranded coiled-coil with the two complementary charged C-terminal extensions maintained essentially the same stability of the most stable homodimeric coiled-coil (Table 2C) and the second charged extension had no effect on specificity. The question arises as to the role of the second charged segments. Perhaps in the full-length molecule, the negatively charged segment of the Kif3A charged region functions to destabilize its homodimeric neck region while the negatively charged segment of the Kif3B charged region functions to destabilize its homodimeric stalk region. In the heterodimer the positively charged regions neutralize the destabilizing effect of the negatively charged regions adjacent to the neck and stalk regions.

The results of a previous study (12), which makes use of truncated mutants of Xlklp3A and Xlklp3B (*Xenopus laevis* kinesin-like protein subunits 3A and 3B), homologous to the neck and highly charged regions of Kif3A and Kif3B, respectively, demonstrated the ability of the C-terminal heptads of the stalk domain to form heterodimers. It was shown that heterodimers could form between the C-terminal regions of the stalks in the absence of the highly charged regions (12). When the investigators used full-length XlKlp3A protein, and a C-terminally truncated XlKlp3B (and vice versa) protein that still had the complementary charged region present, they were not able to detect heterodimers, but this can be explained by their results pertaining to the C-terminal region of the stalk. Thus, these investigators found that there was a distinct need for the C-terminal portion of the stalk domain for the two proteins to bind together so that they could be immunoprecipitated. Hence, the inability of the investigators' C-terminally truncated mutants to form heterodimers with a full-length partner does not preclude the importance of the complementary charged regions described in the present study in heterodimer formation. The complementary charged regions may simply be one component in a two-component system that favors heterodimer formation. The C-terminal heptads of the stalk could be important for binding and specificity, while the complementary charged regions next to the neck coiled-coil could further increase binding specificity. These two regions could work in concert to control/modulate heterodimer formation.

This study clearly demonstrates the importance of highly charged unstructured regions in protein structure and function.

Acknowledgements

This work was supported by NIH grants R01GM 61855 and PO1 AI059576 to R.S.H., the John Stewart Chair in Peptide Chemistry and the University of Colorado Health Sciences Center.

References

1. Bloom GS, Wagner MC, Pfister KK, Brady ST. Native structure and physical properties of bovine brain kinesin and identification of the ATP-binding subunit polypeptide. Biochemistry 1988;27:3409–3416. [PubMed: 3134048]
2. Kuznetsov SA, Vaisberg EA, Shanina NA, Magretova NN, Chernyak VY, Gelfand VI. The quaternary structure of bovine brain kinesin. EMBO J 1988;7:353–356. [PubMed: 3130248]
3. Hirokawa N, Pfister KK, Yorifuji H, Wagner MC, Brady ST, Bloom GS. Submolecular domains of bovine brain kinesin identified by electron microscopy and monoclonal antibody decoration. Cell 1989;56:867–878. [PubMed: 2522351]
4. Wedaman KP, Meyer DW, Rashid DJ, Cole DG, Scholey JM. Sequence and submolecular localization of the 115-kD accessory subunit of the heterotrimeric kinesin-II (KRP85/95) complex. J Cell Biol 1996;132:371–380. [PubMed: 8636215]
5. Yamazaki H, Nakata T, Okada Y, Hirokawa N. Cloning and characterization of KAP3: a novel kinesin superfamily-associated protein of Kif3A/ Kif3B. *Proc.* Natl Acad Sci USA 1996;93:8443–8448.

NIH-PA Author Manuscript

NIH-PA Author Manuscript

NIH-PA Author Manuscript

6. Cole DG, Chinn SW, Wedaman KP, Hall K, Vuong T, Scholey JM. Novel heterotrimeric kinesin-related protein purified from sea urchin eggs. Nature 1993;366:268–270. [PubMed: 8232586]
7. Kondo S, Sato-Yoshitake R, Noda Y, Aizawa H, Nakata T, Matsuura Y, Hirokawa N. Kif3A is a new microtubule-based anterograde motor in the nerve axon. J Cell Biol 1994;125:1095–1107. [PubMed: 7515068]
8. Rashid DJ, Wedaman KP, Scholey JM. Heterodimerization of the two motor subunits of the heterotrimeric kinesin, KRP85/95. J Mol Biol 1995;252:157–162. [PubMed: 7674298]
9. Yamazaki H, Nakata T, Okada Y, Hirokawa N. Kif3A/B: a heterodimeric kinesin superfamily protein that works as a microtubule plus enddirected motor for membrane organelle transport. J Cell Biol 1995;130:1387–1399. [PubMed: 7559760]
10. de Cuevas M, Tao T, Goldstein L. Evidence that the stalk of *Drosophila* kinesin heavy chain is an α-helical coiled-coil. J Cell Biol 1992;116:957–965. [PubMed: 1734025]
11. Hodges RS, Sodek J, Smillie LB, Jurasek L. Tropomyosin: amino acid sequence and coiled-coil structure, Cold Spring Harbor Symp. Quant Biol 1972;37:299–310.
12. De Marco V, Burkhard P, Le Bot N, Vernos I, Hoenger A. Analysis of heterodimer formation by Xklp3A/B, a newly cloned kinesin-II from *Xenopus laevis.* EMBO J 2001;20:3370–3379. [PubMed: 11432825]
13. Chana MS, Tripet BP, Mant CT, Hodges RS. The role of unstructured highly charged regions on the stability and specificity of dimerization of two-stranded α-helical coiled-coils: analysis of the neckhinge region of the kinesin-like motor protein Kif3A. *J. Struct.* Biol 2002;137:206–219.
14. Chana, M.S., Tripet, B.P., Mant, C.T. & Hodges, R.S. (in press) An investigation into the effects of highly charged regions on the stability of the neck region coiled-coil of kinesin-like motor protein Kif3B. *J. Prot. Pept. Lett.* (in press).
15. Merrifield B. Concept and early development of solid-phase peptide synthesis. Meth Enzymol 1997;289:3–13. [PubMed: 9353714]
16. Sereda TJ, Mant CT, Quinn AM, Hodges RS. Effect of the α-amino group on peptide retention behaviour in reversed-phase chromatography. Determination of the pKa values of the α-amino group of 19 different N-terminal amino acid residues. J Chromatogr 1993;646:17–30. [PubMed: 8408425]
17. Fontenot JD, Ball JM, Miller MA, David CM, Montelaro RC. A survey of potential problems and quality control in peptide synthesis by the fluoroenylmethoxycarbonyl procedure. J Pept Res 1991;1:19–25.
18. Stewart, J.M. & Young, J.D. (1984) *Solidphase Peptide Synthesis* Pierce Chemical Company, Rockford, IL.
19. Monera OD, Zhou NE, Kay CM, Hodges RS. Comparison of antiparallel and parallel two-stranded α-helical coiled-coils. Design, synthesis and characterization. J Biol Chem 1993;268:19218–19277. [PubMed: 8366074]
20. O'Shea EK, Rutkowski R, Stafford WF, Kim PS. Preferential heterodimer formation by isolated leucine zippers from Fos and Jun. Science 1989;245:646–648. [PubMed: 2503872]
21. Lavigne P, Kondejewski LH, Houston ME, Sonnichsen RD, Lix B, Sykes BD, Hodges RS. Preferential heterodimeric parallel coiled-coil formation by synthetic max and c-Myc leucine zippers: A description of putative electrostatic interactions responsible for the specificity of heterodimerization. J Mol Biol 1995;254:505–520. [PubMed: 7490766]
22. Gans PJ, Lyu PC, Manning MC, Woody RW, Kallenbach NR. The helix-coil transition in heterogeneous peptides with specific side-chain interactions: theory and comparison with CD spectral data. Biopolymers 1991;31:1605–1614. [PubMed: 1814507]
23. Lau SYM, Taneja AK, Hodges RS. Synthesis of a model protein of defined secondary and quaternary structure: effect of chain length on the stabilization and formation of two-stranded α-helical coiled-coils. J Biol Chem 1984;259:13253–13261. [PubMed: 6490655]
24. Lau SYM, Taneja AK, Hodges RS. Effects of solvents and hydrophobic supports on the secondary and quaternary structure of a model protein: reversed-phase and size-exclusion high performance liquid chromatography. J Chromatogr 1984;317:129–140.
25. Zhou NE, Kay CM, Hodges RS. Synthetic model proteins: the relative contribution of leucine residues at the nonequivalent positions of the 3–4 hydrophobic repeat to the stability of the two-stranded α-helical coiled-coil. Biochemistry 1992;31:5739–5746. [PubMed: 1610823]

NIH-PA Author Manuscript

NIH-PA Author Manuscript

NIH-PA Author Manuscript

26. Zhou NE, Kay CM, Hodges RS. Synthetic model proteins. Positional effects of interchain hydrophobic interactions on stability of two-stranded α-helical coiled-coils. J Biol Chem 1992;267:2664–2670. [PubMed: 1733963]
27. Mant CT, Chao H, Hodges RS. Effect of mobile phase on the oligomerization state of α-helical coiled-coil peptides during high-performance sizeexclusion chromatography. J Chromatogr A 1997;791:85–98. [PubMed: 9463895]
28. Monera OD, Kay CM, Hodges RS. Protein denaturation with guanidine hydrochloride or urea provides a different estimate of stability depending on the contributions of electrostatic interactions. Prot Sci 1994a;3:1984–1991.
29. Schreiber G, Fersht AR. Rapid, electrostatically assisted association of proteins. Nat Struct Biol 1996;3:427–431. [PubMed: 8612072]
30. Kohn WD, Kay CM, Hodges RS. Salt effects on protein stability: twostranded α-helical coiled-coils containing inter- or intrahelical ion-pairs. J Mol Biol 1997;267:1039–1052. [PubMed: 9135129]
31. Hagihara Y, Tan Y, Goto Y. Comparison of the conformational stability of the molten globule and native states of horse cytochrome c. J Mol Biol 1994;237:336–348. [PubMed: 8145245]
32. Kohn WD, Kay CM, Hodges RS. Protein destabilization by electrostatic repulsions in the two-stranded α-helical coiled-coil/leucine zipper. Prot Sci 1995;4:237–250.
33. Kohn WD, Monera OD, Kay CM, Hodges RS. Effects of interhelical repulsions between glutamic acid residues in controlling the dimerization and stability of two-stranded α-helical coiled-coils. J Biol Chem 1995;270:25495–25506. [PubMed: 7592719]
34. Monera OD, Kay CM, Hodges RS. Electrostatic interactions control the parallel and antiparallel orientation of α-helical chains in two-stranded α-helical coiled-coils. Biochemistry 1994;33:3862–3871. [PubMed: 8142389]

NIH-PA Author Manuscript

NIH-PA Author Manuscript

NIH-PA Author Manuscript

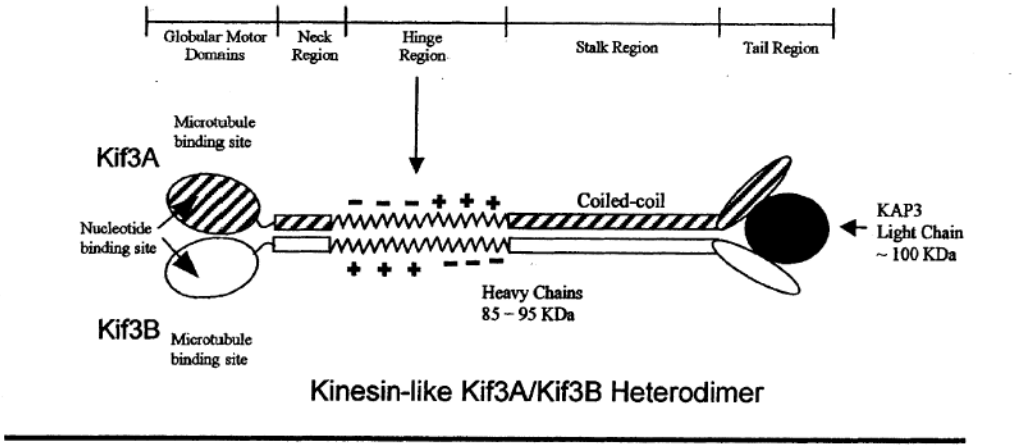

Protein	Peptide name	Res. #	Complementary Charge-Rich Regions
Kif3A Charged Region	**P5**	(378-416)	**Ac**-CGGEEVSGSDISGSEEDDEEGELGEDGEKRKKRRDQAGKKKV-**amide**
Kif3B Charged Region	**P10**	(373-411)	**Ac**-CGGSIGRRKRREKRREGGGSGGGGEEEEEEGEEGEEDGDDKD-**amide**

Figure 1.

Top panel shows a schematic of the kinesin-like heterotrimeric motor protein Kif3A/Kif3B/KAP3. This protein consists of two different polypeptide chains, Kif3A and Kif3B, which resemble conventional kinesin heavy chains. Each polypeptide chain contains a N-terminal globular motor domain, followed by a potential neck coiled-coil region, a highly charged hinge region, a coiled-coil stalk region and the C-terminal tail region (which binds to an accessory unit, the kinesin-like associated protein KAP3). Bottom panel shows the amino acid sequences of the complementary charged regions in Kif3A and Kif3B. Shown are the charged regions, residues 378–416 and 373–411, which comprise the non-homologous regions of Kif3A and Kif3B, respectively. The charged region of Kif3A begins with negatively charged amino acids followed by positively charged amino acids; the analogous region in Kif3B begins with a positively charged region followed by a glycine spacer and then a negatively charged region. CGG represents a flexible linker added N-terminally to each peptide. Ac-denotes N^{α}-acetyl and -amide denotes C^{α}-amide.

NIH-PA Author Manuscript

NIH-PA Author Manuscript

NIH-PA Author Manuscript

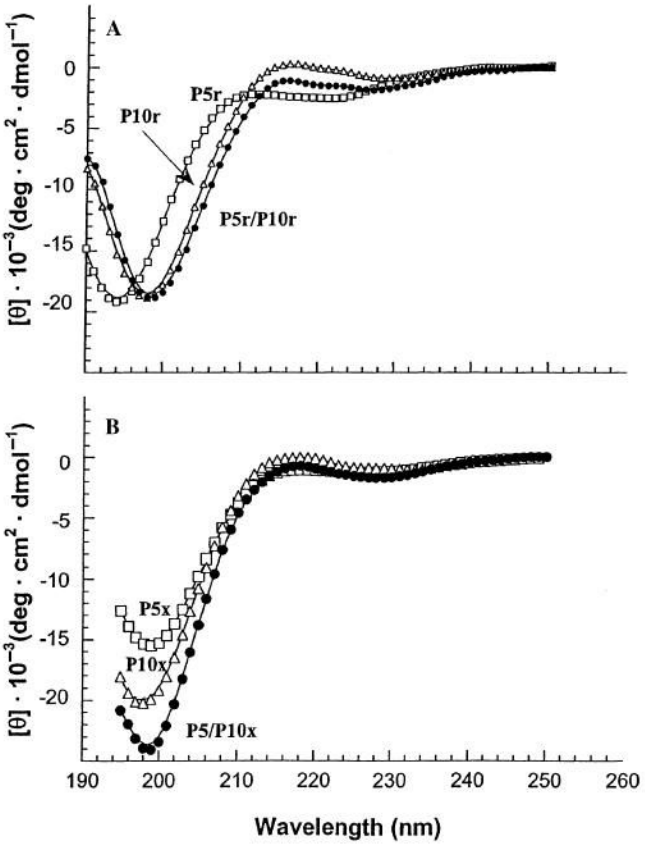

Figure 2.

Circular dichroism (CD) spectra of the complementary charged regions. Panel A depicts the random coil spectra of the non-linked (reduced) peptides denoted P5r, P10r and P5r mixed P10r (1 : 1) denoted P5r/P10r. Panel B shows the random coil spectra of the disulfide-bridged (oxidized) homostranded peptides denoted P5x, P10x and the heterostranded peptide P5/P10x. P5, open squares; P10, open triangles; and P5/P10, closed circles. The peptide sequences are shown in Fig. 3.

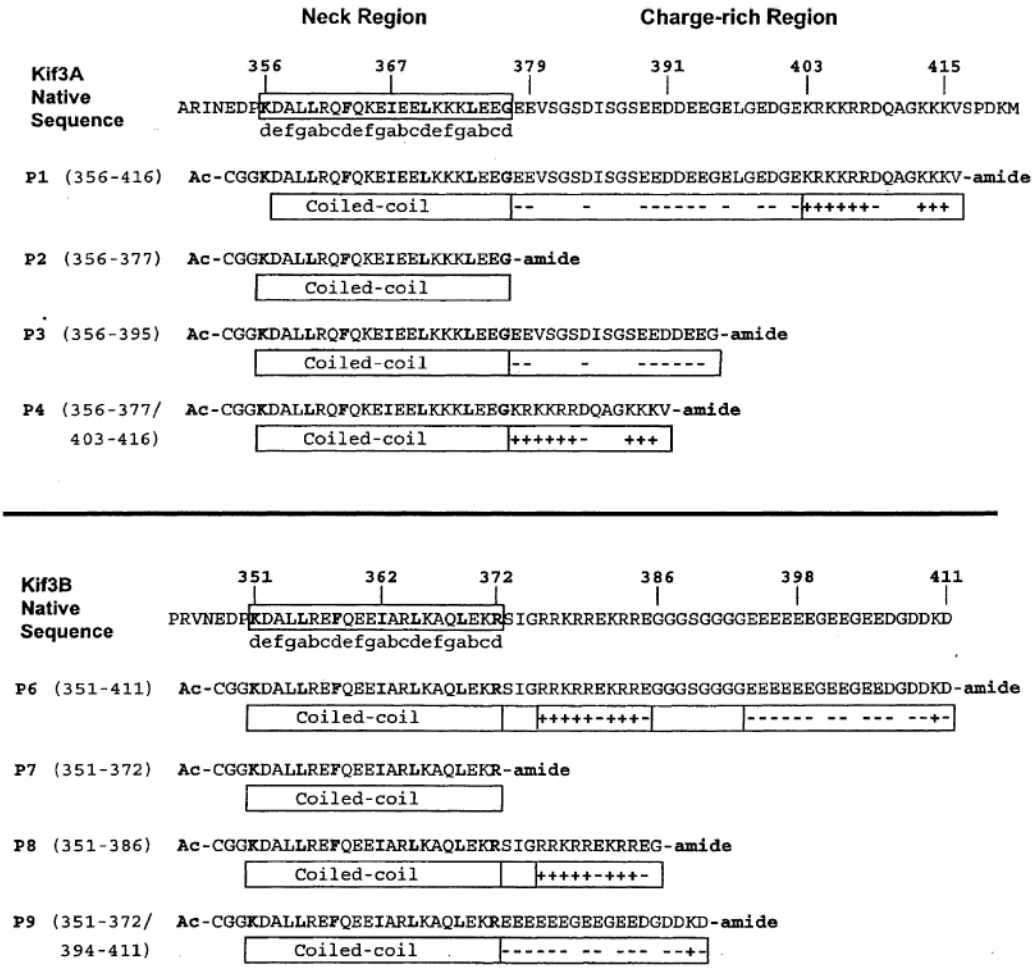

Figure 3.

Amino acid sequences of the Kif3A and Kif3B peptides used in this study. The native mouse Kif3A and Kif3B sequences, residues 356–416 and 351–411, are shown above the synthetic peptides prepared for this study. The open box around the native sequence indicates the predicted neck α-helical coiled-coil region. The heptad repeat of the coiled-coil is denoted by **abcdefg**, where positions **a** and **d** are typically the non-polar residues (shown in bold) involved in the 3–4 hydrophobic repeat. The boxed regions below the peptide sequences denote the predicted coiled-coil region and the highly negatively charged and positively charged regions. The negatively charged residues and positively charged residues are indicated by a (−) or (+) sign, respectively. CGG represents a flexible linker added N-terminally to each peptide. Ac- denotes N^{α}-acetyl and -amide denotes C^{α}-amide. All of the synthetic peptides are aligned to the native sequence except peptides P4 and P9, which consist of coiled-coil regions, residues 356–377 and 351–372, respectively, combined with the positively charged region, residues 403–416, and the negatively charged region, residues 394–411.

NIH-PA Author Manuscript NIH-PA Author Manuscript NIH-PA Author Manuscript

NIH-PA Author Manuscript
NIH-PA Author Manuscript
NIH-PA Author Manuscript

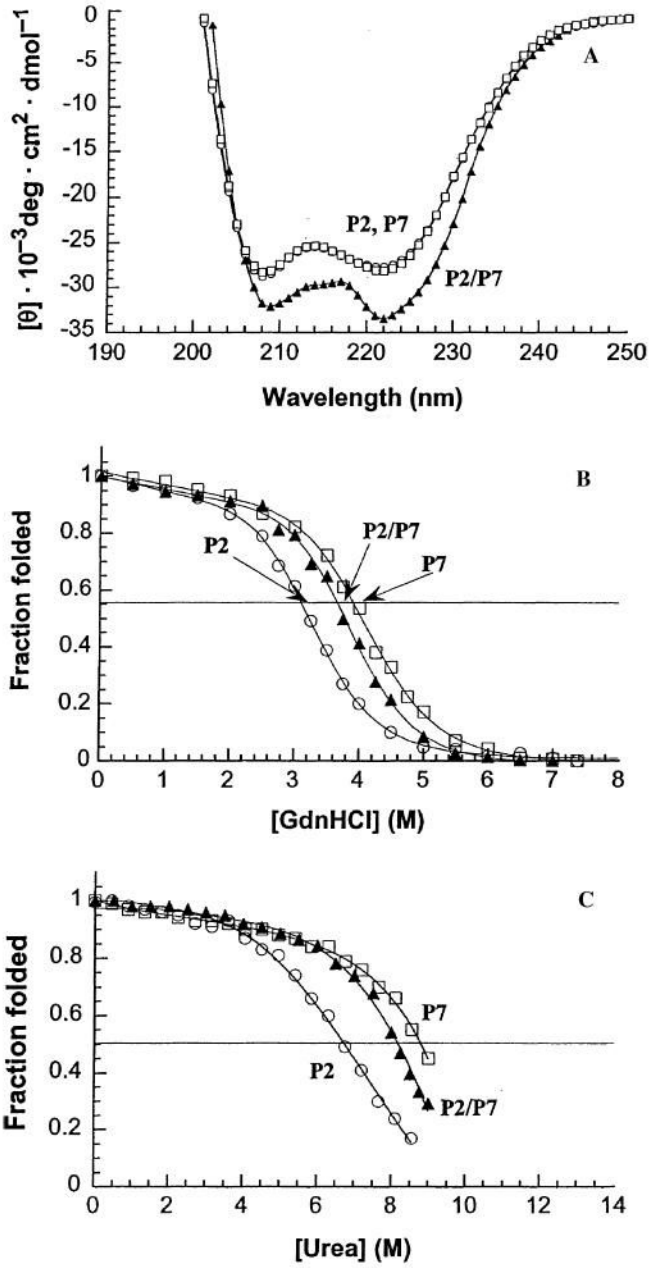

Figure 4.

Comparison of hetero-two-stranded coiled-coil with homo-two-stranded coiled-coil neck regions. Panel A depicts the CD spectra of the three heptad coiled-coils for the neck regions of Kif3A/Kif3B, Kif3A, and Kif3B (peptides P2/P7, P2 and P7, respectively). Panel B depicts the relative stabilities of the neck region coiled-coils in guanidine hydrochloride. Panel C depicts the relative stabilities of the neck region coiled-coils for the homo-and hetero-two-stranded peptides in urea. Homostranded Kif3A neck region, P2, (open circles); homostranded Kif3B neck region, P7, (open squares); heterostranded Kif3A/ Kif3B neck region, P2/P7, (closed triangles). Peptide sequences are shown in Fig. 3.

NIH-PA Author Manuscript

NIH-PA Author Manuscript

NIH-PA Author Manuscript

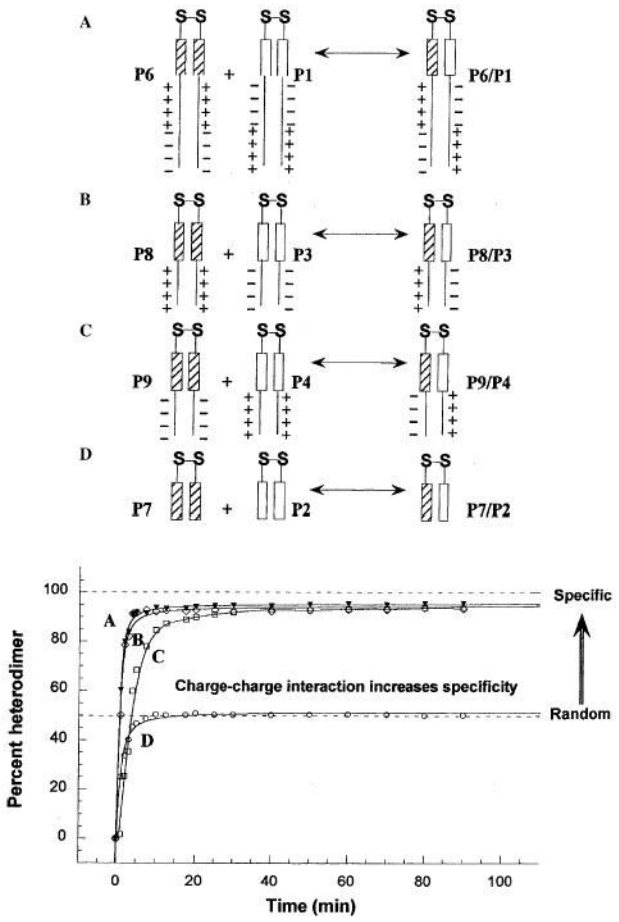

Figure 5.

The formation of oxidized, heterostranded P1/P6, P3/P8, P4/ P9, and P2/P7 from redox experiments as a function of time. Reaction A represents the redox results of oxidized peptides P1 and P6 (closed triangles in plot). Reactions B and C represent the redox reactions of oxidized P3 with P8 and P4 with P9, respectively (open diamonds and open squares). Reaction D represents the redox reaction of peptide P2 with P7 (open circles). The percent heterostranded peptide was calculated by dividing the integrated area of the hetero-two-stranded HPLC peak by the total integrated area of both the homo- and heterostranded peptides for each time point. Peptide sequences are shown in Fig. 3.

NIH-PA Author Manuscript

NIH-PA Author Manuscript

NIH-PA Author Manuscript

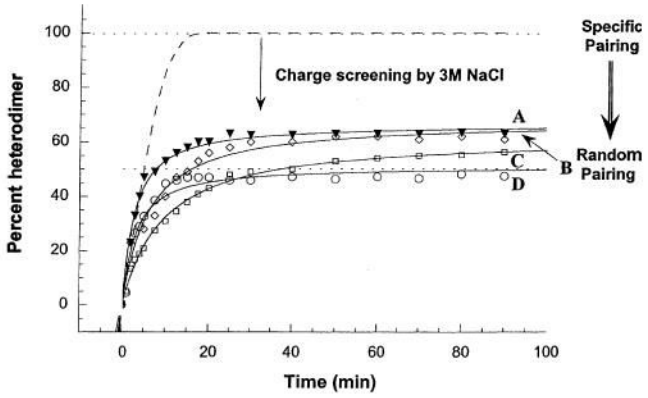

Figure 6.

Formation of heterostranded peptides in the presence of NaCl. The dashed line is the theoretical maximum in benign medium. Reaction A represents the redox results of oxidized peptides P1 and P6 (closed triangles). Reaction B represents the result of mixing oxidized peptides P3 and P8 (open diamonds). Reaction C is the result of mixing oxidized peptides P4 and P9 (open squares). Reaction D is the result of mixing oxidized peptides P2 and P7 (open circles). Percent heterostranded peptide was calculated as described for Fig. 5.

NIH-PA Author Manuscript
NIH-PA Author Manuscript
NIH-PA Author Manuscript

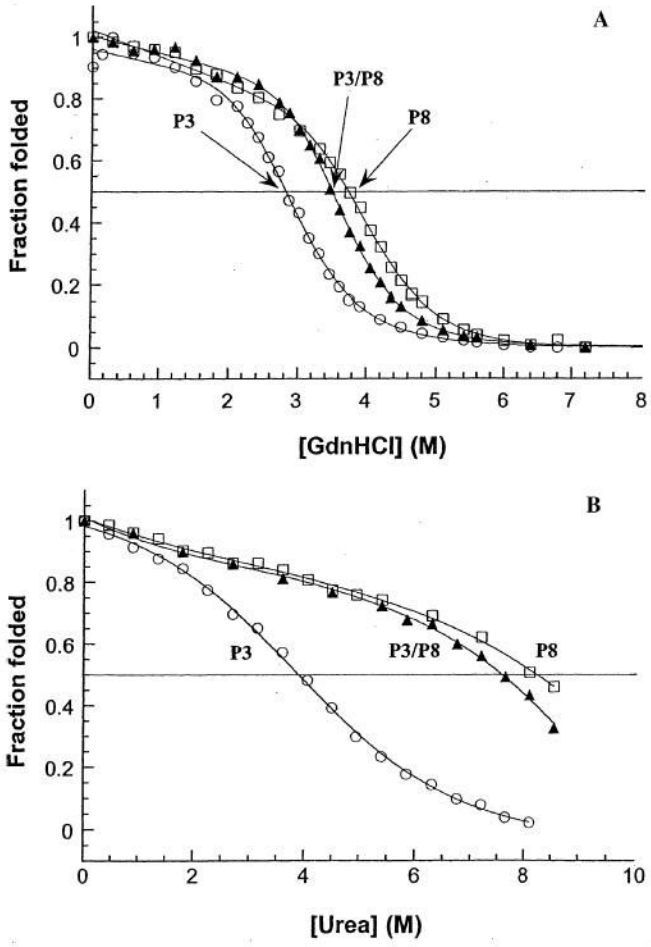

Figure 7.

Comparison of stabilities of oxidized peptides P3, P8, and P3/ P8: coiled-coils with the first segment of the complementary charged region. Panel A depicts the relative stabilities, in guanidine hydrochloride, for homostranded peptide P3, heterostranded peptide P3/P8, and homostranded peptide P8. The peptides are comprised of the neckregion coiled-coils with the first segment from the complementary charged regions found in Kif3A and Kif3B (Fig. 3) added C-terminally. Panel B depicts the relative stabilities of peptides P3, P3/P8, and P8 in urea. Homostranded peptides P3 and P8 (open circles and open squares, respectively); heterostranded peptide P3/P8 (closed triangles). Peptide sequences are shown in Fig. 3.

NIH-PA Author Manuscript
NIH-PA Author Manuscript
NIH-PA Author Manuscript

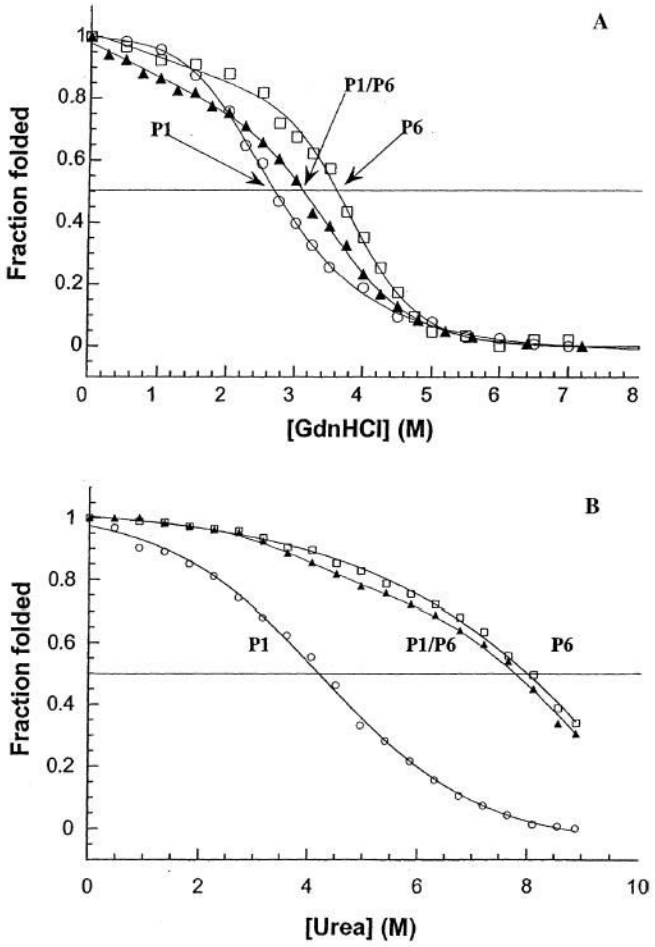

Figure 8.

Comparison of stabilities of oxidized peptides P1, P6, and P1/P6: coiled-coils with both segments of complementary charged residues. Panel A depicts the relative stabilities of the coiled-coil neck regions for homostranded P1, heterostranded P1/P6, and homostranded P6 in guanidine hydrochloride. The peptides are comprised of the coiled-coils with the full complementary charged regions (Fig. 3) added C-terminally. Panel B depicts the stabilities of the peptides in urea. Homostranded peptides P1 and P6 (open circles and open squares, respectively); heterostranded peptide P1/P6 (closed triangles). Peptide sequences are shown in Fig. 3.

NIH-PA Author Manuscript
NIH-PA Author Manuscript
NIH-PA Author Manuscript

Table 1

Circular dichroism data of synthetic peptides

Peptide[a]	Number of residues[b]	$-[\theta]_{222}$ (deg cm^2 dmol^{-1})[c]		% α-helix[d]		Number of calculated helical residues[e]		$[\theta]_{222}/[\theta]_{208}$[f]	
		Benign	50% TFE	Benign	50% TFE	Benign	50% TFE	Benign	50% TFE
P2	22	27 700	28 750	88	91	19	20	0.96	0.86
P7	22	28 150	28 300	89	90	20	20	0.99	0.86
P2/P7	22/22	33 450	31 750	100	100	22	22	1.05	0.86

[a] Disulfide-bridged homostranded peptides P2 and P7. Disulfide-bridged heterostranded peptide P2/P7. The amino acid sequence for each peptide is shown in Fig. 3.

[b] Number of residues per polypeptide chain.

[c] The mean residue molar ellipticities at 222 nm were measured at 25 °C in benign buffer (0.1 M KCl, 0.05 M PO_4, pH 7). For samples containing TFE, the buffer was diluted 1 : 1 (v/v) with TFE.

[d] The percent helical content was calculated from the ratio of the observed $[\theta]_{222}$ value divided by the predicted molar ellipticity × 100. The predicted molar ellipticity was calculated from the equation $[\theta]_{222} = -40 \times 10^3 \times (1-4.6/n)$ for the chain length dependence of an α-helix (22), where n is the number of residues in the peptide. A peptide of 22 residues has a predicted molar ellipticity of −31 600.

[e] The number of helical residues was calculated by multiplying the percent α-helix by the number of residues in the polypeptide chain, e.g. for reduced P7 in benign medium 27 700/31 600 × 22 residues = 19 α-helical residues predicted in the coiled-coil.

[f] The molar ellipticity values at 222 and 208 nm for each peptide were used to calculate the ratio $[\theta]_{222}/[\theta]_{208}$.

NIH-PA Author Manuscript

NIH-PA Author Manuscript

NIH-PA Author Manuscript

Table 2

Denaturation data

Peptide[a]	Oxidized	
	GdnHCl[b] $_{1/2}$ (M)	Urea[c] $_{1/2}$ (M)
(A) For synthetic coiled-coil peptides		
P2	3.1	6.7
P7	3.9	8.8
P2/P7	3.6	8.1
(B) For synthetic peptides with one charge segment		
P3	2.8	3.9
P8	3.7	8.2
P3/P8	3.5	7.6
(C) For synthetic peptides with both charge segments		
P1	2.7	3.9
P6	3.6	8.0
P1/P6	3.1	7.8

[a] Disulfide-bridged homostranded peptides P2, P7, P3, P8, P1 and P6. Disulfide-bridged heterostranded peptides P2/P7, P3/P8 and P1/P6. The amino acid sequence for each peptide is shown in Fig. 1.

[b] GdnHCl$_{1/2}$ is the concentration of guanidine hydrochloride (M) required to give a 50% decrease in the molar ellipticity at 222 nm.

[c] Urea$_{1/2}$ is the concentration of urea (M) required to give a 50% decrease in the molar ellipticity at 222 nm.